EPJ Applied Physics proofs
(will be inserted by the editor)

Characteristics of $FeSi_2$ quantum dots on silicon

L. Dózsa[a], E. Horváth, G. Molnár, A. L. Tóth, Z. Vértesy, E. Vázsonyi, and G. Petö

Research Institute for Technical Physics and Materials Science, H-1525 P. O. Box 49, Budapest, Hungary

Received: date / Revised version: date – © EDP Sciences

Abstract. Self-assembled β-$FeSi_2$ quantum (QD) dots were grown on n-type Si and investigated in this work. Secondary electron images show the shape and distribution of the quantum dots depends on the temperature and thickness of the Fe deposition. Electrical characteristics were measured in MIS devices prepared by covering the quantum dots by an oxide or by a photoresist layer. The cold deposited and subsequently annealed Fe layers were found to generate large concentration of deep level defects, compensating the upper few microns layer of the silicon wafer. Reactive deposition epitaxy (RDE) growth of QDs—where the iron is deposited on hot substrate—generated much lower concentration of defect, in some devices with characteristics comparable to the reference wafer. The significant scatter on the surface is attributed to inhomogeneous growth conditions and to residual surface contamination on the surface.

PACS. 81.07.Ta Quantum dots – 71.55.Cn Elemental semiconductors – 73.40.Qv Metal-insulator-semiconductor structures (including semiconductor-to-insulator)

1 Introduction

Metal silicide films have attracted attention because of their scientific curiosity and their technical importance. Their applicability in integrated circuit technology motivated the studies of the properties of different silicides. They have generally metal-like electrical resistivity, exhibit good high temperature stability and oxidation resistance [1].

Iron is a member of the VIIIB group, but Si atoms were found to be the moving species during the growth of FeSi phase [2], in contrast to other near noble metals. β-$FeSi_2$ is a semiconductor with a band gap of 0.87 eV [3]. For this reason it was regarded as a potential material for optoelectronic applications in silicon integrated technology. A lot of efforts have been made to prepare semiconducting epitaxial β-$FeSi_2$ layers [4], whilst less work has been done to understand the basic solid phase reaction of Fe thin film and Si substrate. In [5] the formation kinetics of iron-silicide was investigated, describing compound layers of FeSi and Fe_3Si formed at about 450 °C and $FeSi_2$ formation at about 550 °C. Another paper reported the appearance of FeSi at about 400 °C, and a small amount of Fe_3Si was detected in samples annealed between 450 and 500 °C [6]. The iron-disilicide phase formed at higher temperature and it came to light that the FeSi <=> β-$FeSi_2$ phase transformation is a nucleation controlled process. The nucleation controlled solid phase reactions produce rough surfaces as a consequence of the coalescence of growing nuclei from different spots. To avoid the rough film morphology, the reactive deposition epitaxy (RDE) method was suggested to prepare β-$FeSi_2$ films, where the Fe atoms impinge on a hot substrate [7].

The preparation of artificial low dimension structures for electron confinement is one of the most challenging research fields of the solid state technology [8]. The phenomena of self-assembly have been observed in a wide range of material and substrate combinations [9]. Recently, heteroepitaxial growth of strained semiconductor structures has attracted great interest owing to their scientific curiosity and possible technical importance as QDs [10]. The generated quantum dots, through the combination of growth kinetics and strain effects show a narrow size distribution.

Earlier, a few publications reported island or wire-like aggregations of the silicides on Si substrate. $TiSi_2$ islands were observed both on Si(100) and Si(111) by Ti deposition at elevated temperatures followed by high temperature annealing [11]. $CoSi_2$ nanostructures were prepared on Si(100) by reactive deposition epitaxy and their nucleation and evolution were studied during the annealing [12]. Recently, two groups in case of the rare earth (Er, Dy, Ho) silicides [13,14] reported nanowire formation. Suemasu and coworkers reported the aggregation of monocrystalline β-$FeSi_2$ islands on the top of Si(100) substrate and the spherical transformation of islands inside a Si overlayer [15].

The motivation of the recent study was to demonstrate the possibility of self-assembled epitaxial β-$FeSi_2$ quantum dot formation on Si(100) substrates, and to follow the evolution of QD growth as a function of film thickness, and to measure the effect of QDs on the electrical characteristics of MIS structures.

[a] e-mail: dozsa@mfa.kfki.hu

2 Sample preparation and experiment

N-type 280±15 μm thick, (100) oriented Si wafers were used as substrates. Their backside was implanted by $P_{31}{}^{+}$ ions (40 keV, 480 °C), cleaned by plasma and wet processes, and annealed at 900 °C for 30 min in N_2 ambient. Before loading the samples into the oil free evaporation chamber (VARIAN VT-460), the native oxide was removed using dilute HF. The time elapsed after cleaning to reach 1 Pa pressure in the vacuum chamber was about 30 min. After evacuation down to $1^{*}10^{-6}$ Pa and prior to evaporation, the Si wafers were annealed in situ for 5 min. at 800 °C. Iron ingots of 99.9% purity were evaporated onto room temperature substrate using an electron gun at an evaporation rate of 0.02–0.03 nm/s, at a pressure of $3^{*}10^{-6}$ Pa. The film thickness was measured by a vibrating quartz. Immediately after Fe deposition the wafers were annealed by resistively heated tungsten spirals in-situ under $3–6^{*}10^{-6}$ Pa pressure. Three types of samples were prepared on Si(100) substrates by evaporating Fe in thickness of 2, 4, and 7 nm. The samples were annealed at 600 °C for 10 minutes.

RDE growth reduces the inhomogeneity caused by the nucleation-dominated character of the FeSi $\Leftrightarrow$ β-$FeSi_2$ reaction [12]. The RDE QDs were grown by evaporating 2 nm and 5 nm Fe at 0.015 nm/s rate onto the 600 °C Si(100) substrate. After evaporation it was annealed further for 5 min at the same temperature.

In order to measure the effect of QD growth on the electrical characteristics the QDs were covered by 100 nm Balzers SiO powder or by 0.5 μm photoresist. After dehydration at 120 °C the the Shipley 1805 photoresist layer was deposited at 4000 r/m spin speed, soft baked at 90 °C, and hard baked at 120 °C. Aluminum dots were evaporated on the oxide and photoresist layers to form MIS structures for the electric characterisation. A reference MIS structure was prepared without Fe deposition.

The samples were measured by X-ray diffraction, by electron microscopy, by current-voltage (I-V), by capacitance-voltage (C-V) measurements, and by DLTS. The secondary electron images were taken by a LEO Gemini 1540 scanning electron microscope. The C-V characteristics were measured in a computer controlled Boonton bridge based setup. The I-V measurements were carried out in a Keithley 236 source-measure unit in the 80–350 K range with better than 0.1 K stability. DLTS was measured in a SEMILAB 83D system.

3 Results

The X-ray diffraction shows the main component of the grown material is β-$FeSi_{2.}$, in agreement with earlier experiments [7]. The secondary electron image in. Figure 1a shows the QDs on 2 nm cold Fe deposited wafer. The lateral dimensions and density of the QDs is in the 4 nm Fe thickness samples, and the image contrast is improved. In Figure 1b the QDs grown from 7 nm cold deposited Fe samples are shown. The height of the QDs is increasing, and the QDs do not grow homogeneously. In the positions between large QDs new, small dots appear in nucleation sites. The secondary electron images of RDE QDs grown from 2 and 5 nm Fe are shown in Figure 1c and d, respectively. In Figure 1d the magnification is 3 times lower. In Figure 1c the QDs are small elongated while in Figure 1d are definitely larger, with significant scatter. The spot-size histogramms were used to numerically describe these features.

The I-V measurements in the photoresist MIS structures and in the oxide covered 7 nm cold iron deposited MIS samples have shown few μA forward current. Typical C-V characteristics in the oxide-covered cold Fe evaporated and the RDE structures are shown in Figure 2a and b, respectively. The dotted lines show tha values measured under illumination. Measurements on four samples devices are shown in all structures to illustrate the scatter. The effect is smaller photoresist samples. The smaller capacitance in Figure 2a is due to compensation of the Si wafer doping (2×10^{15}/ cm^3) by the generated point defects. Thicker Fe layer compensate the Si substrate into larger depth. In RDE QD structures the capacitance is large, in some samples it is comparable to the reference samples, indicating that much less point defects generated by the RDE growth. The significant scatter is due to homogeneous growth conditions on the surface. The measured devices are not comparable to a MOS structure, due to the high contamination by Fe at the interface, its purpose is to reduce the direct short-curcuiting of the barrier, and to make possible the estimate the demage generated by the Fe-Si reaction. The presence of the inversion layer can be observed, mainly in the RDe and reference samples at low temparature.

DLTS were measured at -4 V reverse bias, with 0 V excitation pulses of 200 μs length, at 160/s repetition rate. The DLTS spectra are shown in Figure 3a. In the cold Fe evaporated samples the peaks were broad and small amplitude, in the RDE samples samples and in reference samples large peaks were found. The temperature dependence at the reverse bias of the DLTS measurement is shown in Figure 3b. The peaks are not related to point defects, but to a balance of the generation-inversion at the oxide-silicon interface, and to a pronounced compensated silicon layer in the cold deposited samples.

4 Conclusion

$FeSi_2$ QDs prepared by annealing cold deposited Fe layers and by RDE deposition of Fe layers were investigated. Secondary electron images have shown the QD density and its size scatter increases above above a critical thickness, due to new nucleation sites. In the RDE grown samples in thick Fe layers resulted in large, irregular size QD growth. The electrical characteristics of MIS structures have shown the cold deposited Fe layers during generated larger than 2×10^{15}/ cm^3 concentration of defect, compensating the silicon wafer near the surface. The nature of the compensating defect could not be identified by DLTS due to its huge concentration. DLTS spectra in the RDE

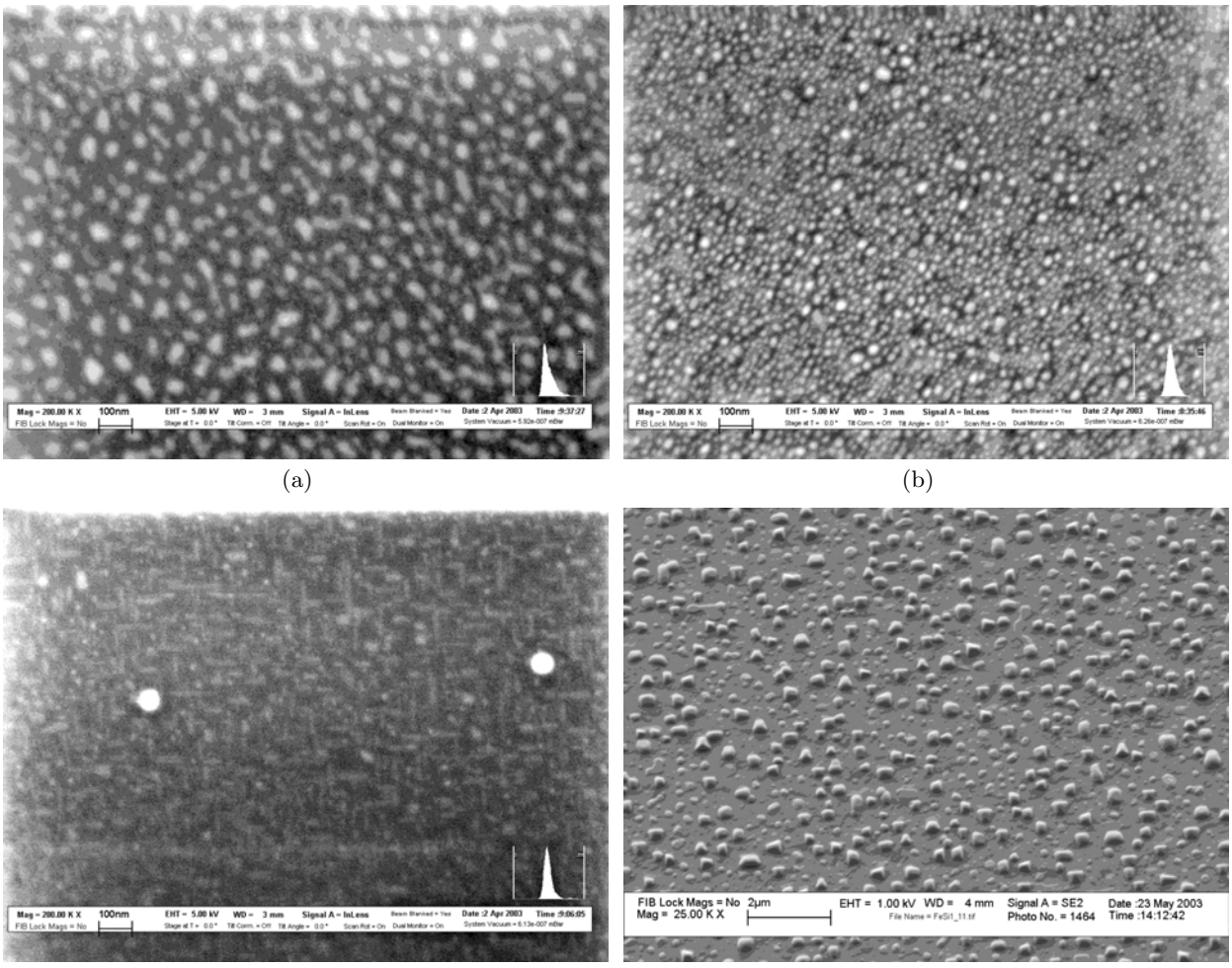

Fig. 1. Secondary electron images of the $FeSi_2$ quantum dots prepared by annealing of cold deposited 2 nm Fe (a) and 7 nm Fe (b), and by RDE deposition of 2 nm Fe (c) and 5 nm Fe (d).

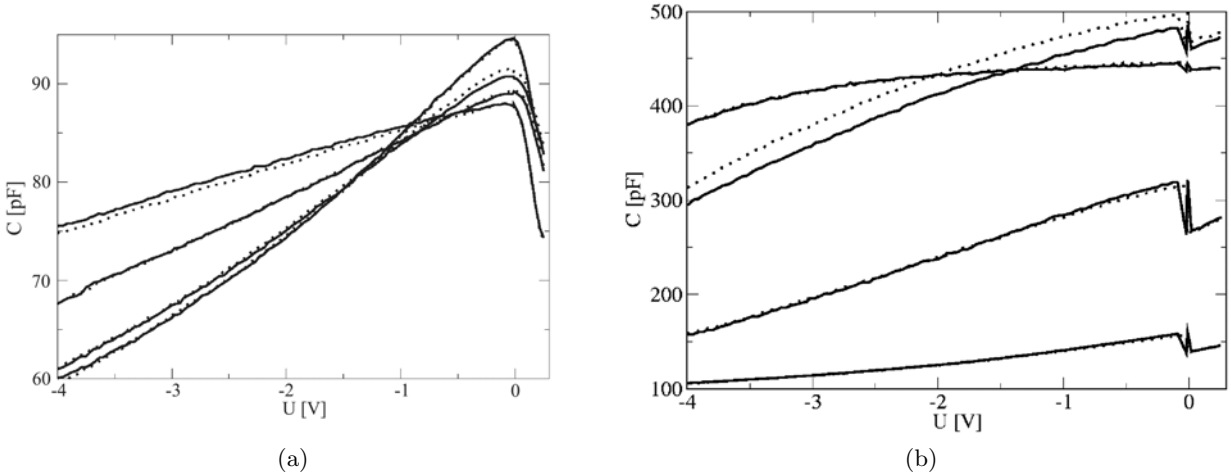

(a) (b)

Fig. 2. C-V plots measured at room temperature in four samples in cold Fe deposited (a) and in RDE deposited (b) oxide covered MIS structures. The dotted lines show the plots measured under illumination.

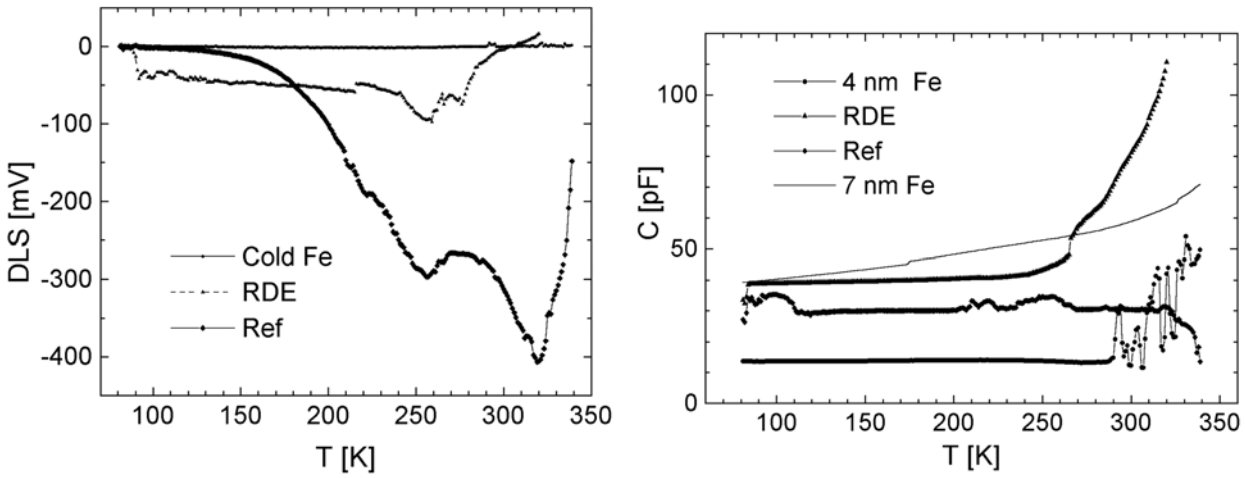

(a) (b)

Fig. 3. DLTS measured at −4 V reverse bias, 0 V, 200 μs excitation pulses, at 160/s repetition rate (a) and temperature dependence of the capacitance measured at −4 V during the DLTS scan is shown (b).

grown QD samples show defects similar to reference samples, so these defects are not related to QD states, but to the residual surface contamination. The large scatter in characteristics indicates the growth parameters are not homogenous on the surface.

The work was partly supported by the Hungarian National Research Fund (OTKA) grants T-30419, and T-035273.

References

1. A. H. Reader, A. H. van Ommen, P. J. W. Weijs, R. A. M. Wolters, D. J. Oostra, Rep. Prog. Phys. **56**, 1397 (1992)
2. W. K. Chu, S. S. Lau, J. W. Mayer, H. Müller, K. N. Tu, Thin Solid Films **25**, 393 (1975)
3. Bost, J. E. Mahan, J. Appl. Phys. **64**, 2034 (1988)
4. J. E. Mahan, K. M. Geib, G. Y. Robinson, R. G. Long, Y. Xinghua, G. Bai, M. A. Nicolet, M. Nathan, Appl. Phys. Lett. **56**, 2126 (1990)
5. S. S. Lau, J. S.-Y. Feng, J. O. Olowolafe, M.-A. Nicolet, Thin Solid Films **25**, 415 (1975)
6. H. C. Cheng, T. R. Yew, L. J. Chen, J. Appl. Phys. **57**, 5246 (1985)
7. G. Molnár, G. Petö, E. Zsoldos, Z. E. Horváth, N. Q. Khanh, Mat. Res. Symp. Proc. **402**, 337 (1996)
8. L. Jacak, Eur. J. Phys. **21**, 487 (2000)
9. V. A. Schukin, D. Bimberg, Appl. Phys. A **67**, 687 (1998)
10. A.-L. Barabási, Appl. Phys. Lett. **70**, 2565 (1997)
11. T. I. Kamins, R. S. Williams, Y. Chen, Y. L. Chang, Y. A. Chang, Appl. Phys. Lett. **76**, 562 (2000)
12. I. Goldfarb, G. A. D. Briggs, Phys. Rev. B **60**, 4800 (1999)
13. Y. Chen, D. A. A. Ohlberg, G. Medeiros-Ribeiro, Y. A. Chang, R. S. Williams, Appl. Phys. Lett. **76**, 4004 (2000)
14. J. Nogami, B. Z. Liu, M. V. Katkov, C. Ohbuchi, N. O. Birge, Phys. Rev. B **63**, 233305 (2001)
15. T. Suemasu, M. Tanaka, T. Fujii, S. Hashimoto, Y. Kumagai, F. Hasegawa. Jpn. J. Appl. Phys. **36**, L1225 (1997)